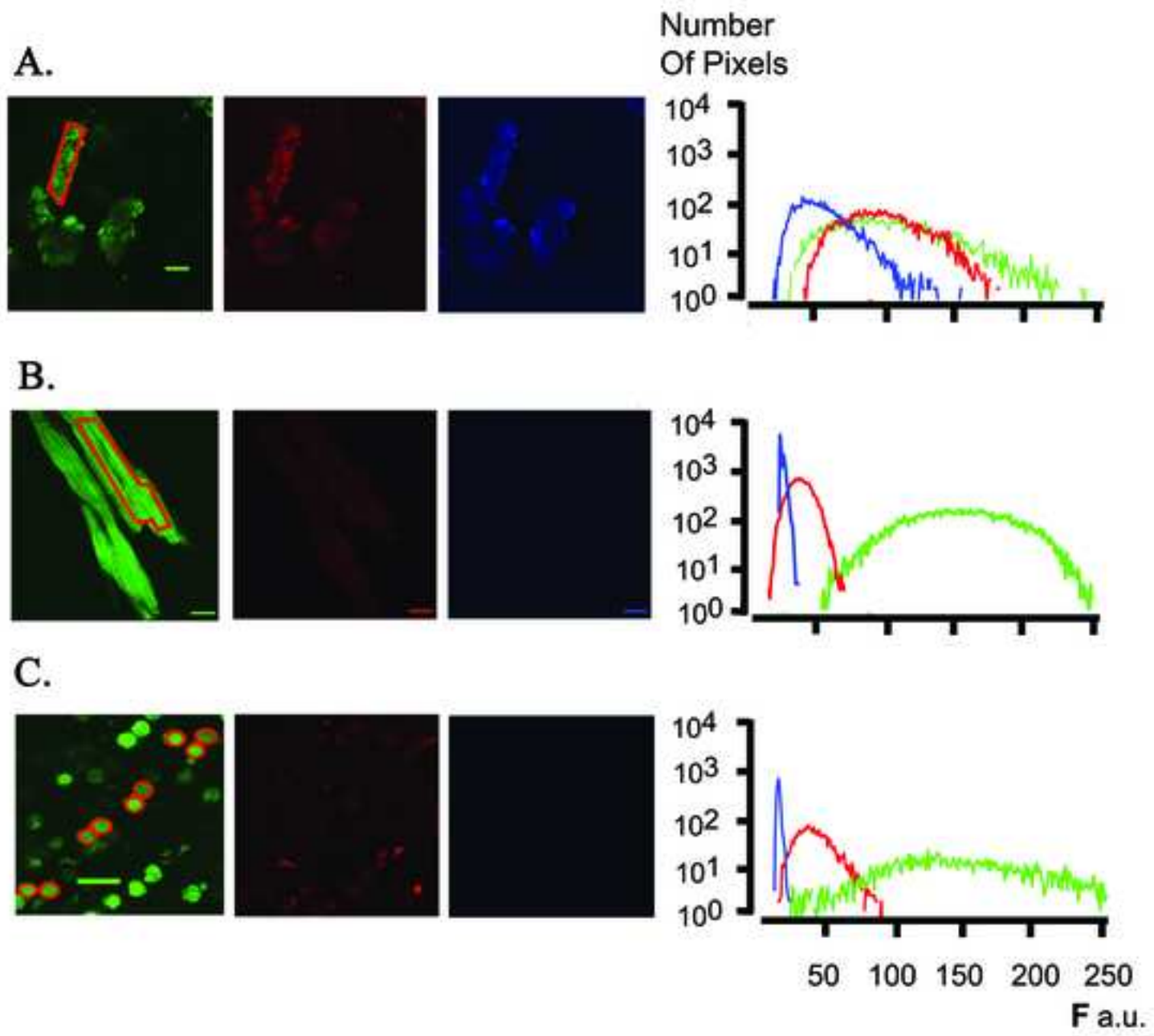
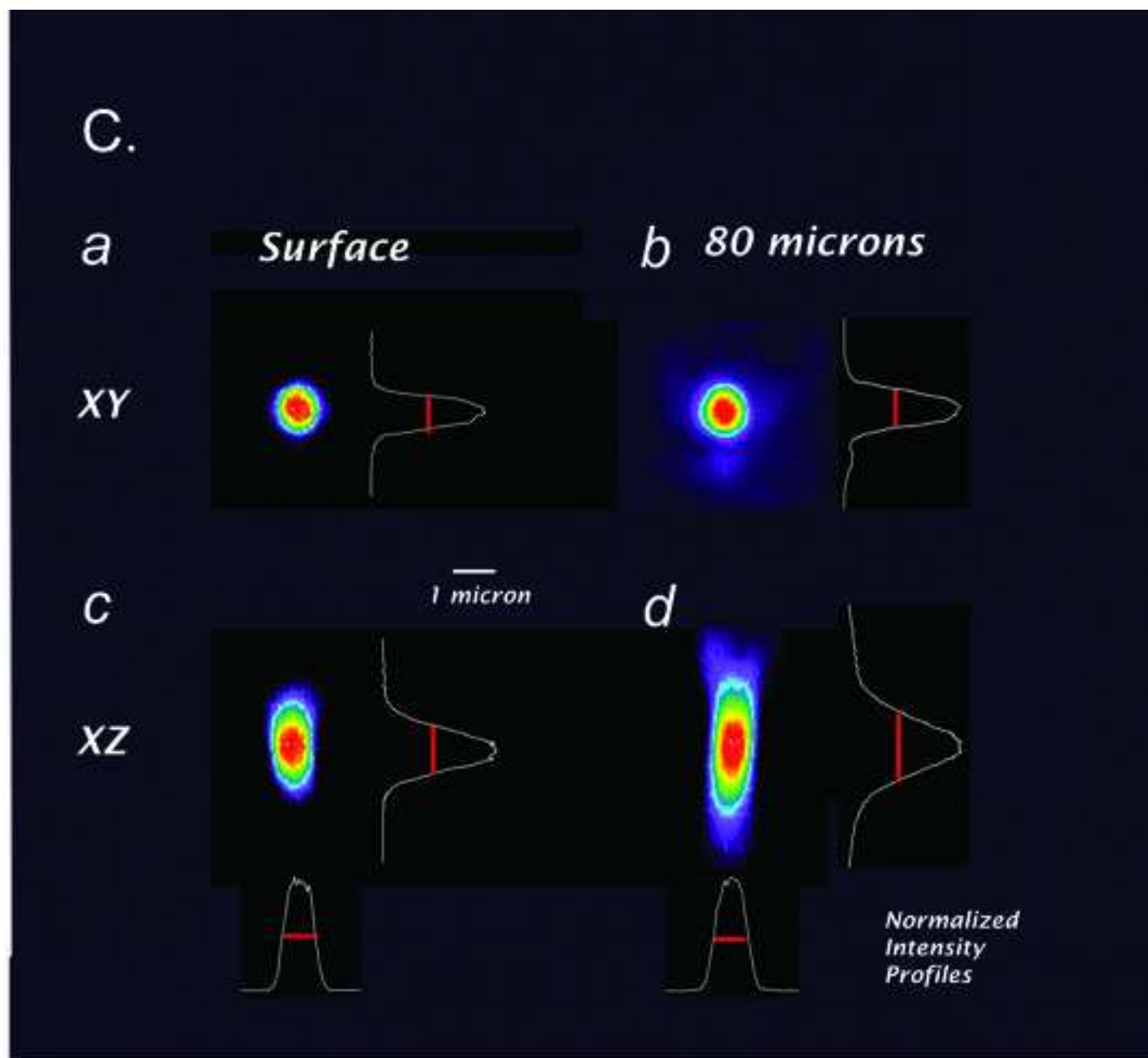


Supplemental Figure 1



Supplementary Figure 2



Supplemental Figure 3

Supplementary Data

Imaging of intracellular calcium transients using TPLSM

Preparation of the hearts carrying bone marrow cell grafts and two-photon laser scanning microscopy (TPLSM) imaging were performed as described previously.^{1,2} Hearts were heparinized, cannulated, and perfused with Tyrode's solution in Langendorff mode. After an initial period of \approx 30 minutes, the perfusion was switched to Tyrode's solution containing the acetoxymethylester (AM) of the calcium fluorophore, rhod-2 (10 μ mol/L; Molecular Probes). After a 15-minute loading period, the perfusion was reverted to dye-free Tyrode's solution to wash out rhod-2 and to allow for a 20-minute incubation period, and the hearts were placed on the microscope stage.

Images were recorded with an MRC 1024 laser scanning microscope (Bio-Rad Laboratories Inc., Hercules, CA) modified for two-photon excitation. Illumination for two-photon excitation was provided by a mode-locked Ti:sapphire laser (Spectra-Physics Laser, Irvine, CA); the excitation wavelength was 810 nm. Hearts were imaged through a uniformly illuminated Nikon x60 1.2 numerical aperture water-immersion lens with a working distance of 200 μ m. Emitted light was collected in the non-descanned mode (i.e., in the absence of a pinhole in the detection path³) by three photo-multiplier tubes fitted with narrow bandwidth filters for 560–650 nm, 500–550 nm, and 450–500 nm, respectively. Scanning was performed in the full frame- and line-mode of the imaging system. For full-frame mode analyses, hearts were scanned at 1.46 and 0.73 frames per second on horizontal (X , Y) planes. For line-scan mode analyses, hearts were scanned repetitively at a rate of 500 Hz and line-scan images were constructed by stacking all lines vertically. Images were obtained at depths of up to 100 μ m below the epicardial surface. All resulting images were digitized at 8-bit resolution and stored directly on the hard

disk. Post-acquisition analysis was performed using MetaMorph software version 4.6 (Molecular Devices, Downingtown, PA).

During TPLSM imaging, hearts were perfused with oxygenated normal Tyrode's solution containing 50 $\mu\text{mol/l}$ cytochalasin D to eliminate contraction-induced movement. Records were made during spontaneous sinus rhythm and/or electrical point stimulation at a site remote from the graft, using square-waved pulses of 2-ms duration and twice diastolic threshold. In some experiments, electrical field stimulation of Langendorff-perfused hearts was performed by positioning the heart between a pair of loop-shaped platinum wires placed approximately 1 cm apart, with the current flowing roughly perpendicular to the longitudinal axis of the heart. The hearts were stimulated with 60- to 100-V pulses of 1- to 2-ms duration using a Grass-Telefactor model SD9 stimulator.

The temporal profiles of intracellular calcium ($[\text{Ca}^{2+}]_i$) transients were obtained by first averaging the line-plot data for each line and then plotting the average intensity per line as a function of time.

Calcium responses in donor-derived cells and host cardiomyocytes were elicited during spontaneous sinus rhythm, electrical point stimulation at a site remote from the graft, and electrical field stimulation. Estimates of the axial resolution of the imaging system in buffer-perfused mouse heart revealed that rhod-2 signals sampled from voxels located within a 5- μm axial distance from the donor-host cell interface represent variable contributions from both cell types. Consequently, the functional status of a cell whose entire volume was located within this critical range was undefined.

Differentiation of green autofluorescence from EGFP fluorescence

We evaluated whether donor-derived cells can be identified by virtue of their green EGFP fluorescence in buffer-perfused, infarcted mouse hearts using TPLSM. Specifically, we were interested in determining whether EGFP can be efficiently discriminated from green autofluorescence, which reportedly can be mistaken as EGFP fluorescence in the ischemically injured heart under epifluorescence illumination.⁴ TPLSM imaging (excitation wavelength, 810 nm) performed in the peri-infarct region of a 10-day-old infarct in a non-transgenic, Langendorff-perfused, adult heart, occasionally revealed polymorphic, strongly autofluorescent structures (Supplementary Fig. 2A). The autofluorescence signal appeared equally strong over the entire emission range as demonstrated by the intensity histograms. In contrast, spectral analyses demonstrated that EGFP robustly fluoresces in the green range and weakly in the red range and not at all in the blue range (Supplementary Fig. 2B; images were obtained from a non-infarcted, Langendorff-perfused transgenic heart expressing EGFP under the control of the cardiomyocyte-specific α -MHC promoter⁵). TPLSM imaging of EGFP-expressing BM cells at 9 days following their transplantation into peri-infarct myocardium of non-transgenic hearts (Supplementary Fig. 2C) demonstrated that the emission profile of EGFP was unaltered compared to that observed in non-infarcted α -MHC-EGFP hearts. Thus, the donor cells exhibit robust expression of EGFP which can be reliably distinguished from injury-induced autofluorescence on the basis of their distinct emission profiles under the vital imaging conditions used in this study. A similar technique had been employed previously to differentiate tissue autofluorescence from EGFP expression in embryonic stem cell-derived cardiomyocytes following their transplantation into infarcted myocardium.⁶

Measurements of the three-dimensional fluorescent profiles of fluorescent spheres in Langendorff-perfused heart

To determine whether a decline in lateral or axial resolution, or both, gives rise to the loss of spatial discrimination in living mouse heart, we examined the three-dimensional fluorescence profile of 1- μm fluorescent spheres with spectral properties similar to those of rhod-2 (excitation 810 nm, emission 560-650 nm) following intracoronary injection into a Langendorff-perfused heart. An X, Y image of a fluorescent sphere obtained at 5 μm below the epicardial surface revealed a perfectly circular cross section (Supplementary Fig. 3). In contrast, the X, Z reconstruction of the same bead revealed deformation into an elongated oval in the z dimension, resulting from spherical aberration. This distortion becomes more accentuated at increasing depth into the specimen. The normalized fluorescence intensity profiles through the center of the microspheres and the corresponding full-width at half maximum fluorescence intensity (FWHM) profiles were essentially identical in the x and y dimensions at either depth (1.46 μm and 1.48 μm , respectively), indicating lack of lateral distortion within the focal plane. The FWHMs in the z direction at 5 and 80 μm were approximately 1.1 and 1.5 times larger, respectively, than the FWHMs in the x and y dimensions. Identical results were obtained in 6 more spheres located between 0-10 and 70-80 μm below the epicardial surface, respectively. Thus, a marked axial broadening of the two-photon excitation volume contributes to the decline of the spatial resolution at depth.

Supplementary Figure Legends

Supplementary Figure 1: Expression levels of different surface markers in *ACT-EGFP* c-kit^{enr} cells expressing EGFP. *ACT-EGFP* low-density BM cells were selected for c-kit⁺ (CD117⁺) cells and stained with different surface markers as described in Materials and Methods. Analysis of GFP expression versus side scatter (SSC) identified 36% of eluted cells as EGFP⁺ (dot plot A). Dot plots B through E depict the expression of four different markers (X axis) versus c-kit expression (Y axis) among eluted, EGFP-expressing cells falling within the low-density mononuclear cell gate. As can be seen in these four dot plots, approximately 72% of the eluted, EGFP-positive cells expressed c-kit (average of percentages in the upper quadrants of B through E). Expression of other markers ranged from approximately 4 % (Flk-1⁺) to 27 % (Sca-1⁺). Percentages shown in the figure were rounded up to the closest integer.

Supplementary Figure 2: Differentiation of cellular autofluorescence from EGFP fluorescence in the infarct border zone. TPLSM frame-mode images obtained from (A) the infarct border zone of an adult non-transgenic heart at 10 days following ligation of the left anterior descending coronary artery, (B) an adult, uninjured heart expressing EGFP under the control of the cardiomyocyte-specific α -MHC promoter,⁵ and (C) EGFP-expressing lin⁻ c-kit⁺ BM cells 9 days following transplantation into the peri-infarct zone of a non-transgenic heart. Excitation wavelength was 810 nm. Fluorescence was simultaneously collected in the red (560-650 nm), green (500-550 nm), and blue (440 -470 nm) range. Photomultipliers of all three emission channels were set at equivalent values for gain and offset. Fluorescence intensity histograms from the outlined regions in the TPLSM images are shown on the right. Y axes are log-scaled. Blue colored curves in panels B and C correspond to background signals in the 440-470-nm emission range. Scale bars, 20 μ m. F, fluorescence; a.u., arbitrary units.

Supplementary Figure 3: Degradation of axial discrimination at depth in buffer-perfused mouse heart. Two-photon imaging of 1.0- μm Nile Red fluorescent microspheres in Langendorff-perfused mouse heart. Microspheres were suspended in 1 mL buffer solution and injected into the coronary circulation via a side port in the bubble trap of the perfusion apparatus. A fraction of the beads became entrapped in the capillaries and were used for imaging. The perfusate was supplemented with 50 mmol/L 2,3 butanedione monoxime to uncouple excitation and contraction.⁷ Microspheres were optically sectioned by recording x, y scans at 0.1- μm axial steps. (**a** and **b**) x, y Maximum projection images of two fluorescent spheres at the focus depths indicated. (**c** and **d**) x, z reconstructions of the same spheres shown in *a* and *b*. Graphs in panels *a* to *d* illustrate the normalized intensity profiles recorded from the maximum projections of the microspheres. Red lines in the intensity profiles indicate the full width at half-maximum fluorescence intensity. Images were obtained with a Nikon 60x water immersion objective with a numerical aperture of 1.2 at a pixel resolution of 0.1 μm and z -steps of 0.1 μm with a Kalman 3 filter. The excitation wavelength was 810 nm and emission was collected in the 560-650 nm range in non-descanned mode of a BioRad1024 laser scanning microscope modified for 2-photon illumination.

References for Supplementary Data

1. Rubart M, Wang E, Dunn KW, Field LJ (2003). Two-photon molecular excitation imaging of Ca^{2+} transients in Langendorff-perfused mouse hearts. *Am J Physiol Cell Physiol*; **284**:C1654-1568.

2. Rubart M, Pasumarthi KB, Nakajima H, Soonpaa MH, Nakajima HO, Field LJ (2003). Physiological coupling of donor and host cardiomyocytes after cellular transplantation. *Circ Res*; **92**:1217-1224.
3. Centonze VE, White JG (1998). Multiphoton excitation provides optical sections from deeper within scattering specimens than confocal imaging. *Biophys J*; **75**:2015-2024.
4. Laflamme MA, Murry CE (2005). Regenerating the heart. *Nat Biotechnol*; **23**:845-856
5. Rubart M, Pasumarthi KB, Nakajima H, Soonpaa MH, Nakajima HO, Field LJ (2003). Physiological coupling of donor and host cardiomyocytes after cellular transplantation. *Circ Res*; **92**:1217-1224.
6. van Laake LW, Passier R, Monshouwer-Kloots J, Nederhoff MG, Ward-van Oostwaard D, Field LJ, *et al.* (2007). Monitoring of cell therapy and assessment of cardiac function using magnetic resonance imaging in a mouse model of myocardial infarction. *Nat Protoc*; **2**:2551-2567.
7. Rubart M, Wang E, Dunn KW, Field LJ (2003). Two-photon molecular excitation imaging of Ca²⁺ transients in Langendorff-perfused mouse hearts. *Am J Physiol Cell Physiol*; **284**:C1654-1568.